

Published in final edited form as:

IEEE J Sel Top Quantum Electron. 2010 May ; 16(3): 493–505. doi:10.1109/JSTQE.2009.2034541.

Review of Neurosurgical Fluorescence Imaging Methodologies

Brian W. Pogue^{1,2}, Summer Gibbs-Strauss⁴, Pablo A. Valdés¹, Kimberley Samkoe¹, David W. Roberts², and Keith D. Paulsen^{1,3}

¹Thayer School of Engineering, Dartmouth College, Hanover NH 03755

²Department of Surgery, Dartmouth Medical School, Lebanon NH 03756

³Department of Diagnostic Radiology, Dartmouth Medical School, Lebanon NH 03756

⁴Beth Israel Deaconess Hospital, Harvard Medical School, Boston MA 02114

Abstract

Fluorescence imaging in neurosurgery has a long historical development, with several different biomarkers and biochemical agents being used, and several technological approaches. This review focuses on the different contrast agents, summarizing endogenous fluorescence, exogenously stimulated fluorescence and exogenous contrast agents, and then on tools used for imaging. It ends with a summary of key clinical trials that lead to consensus studies. The practical utility of protoporphyrin IX (PpIX) as stimulated by administration of δ -aminolevulinic acid (ALA) has had substantial pilot clinical studies and basic science research completed. Recently multi-center clinical trials using PpIX fluorescence to guide resection have shown efficacy for improved short term survival. Exogenous agents are being developed and tested pre-clinically, and hopefully hold the potential for long term survival benefit if they provide additional capabilities for resection of micro-invasive disease or certain tumor sub-types that do not produce PpIX or help delineate low grade tumors. The range of technologies used for measurement and imaging ranges widely, with most clinical trials being carried out with either point probes or modified surgical microscopes. At this point in time, optimized probe approaches are showing efficacy in clinical trials, and fully commercialized imaging systems are emerging, which will clearly help lead to adoption into neurosurgical practice.

Index Terms

brain tumor; glioma; fluorescence; microscopy; imaging; surgery; neurosurgery; protoporphyrin

I. INTRODUCTION

In neurosurgery, the extent of tumor resection plays a significant role in patient prognosis and disease progression, and so maximization of the extent of resection has always been paramount, moderated by the need to not remove areas of normally functioning brain tissue. Fluorescence imaging of brain tumor tissue during resection has been extensively studied as a potential tool to help the neurosurgeon in this process. Although the *in vivo* use of fluorescence in brain tumors dates back to 1948, when Moore reported using fluorescein to image 46 patients with brain tumors [1], it was not until the last decade when a rebirth of this technology took hold in a more widespread manner. Much of the real-time intraoperative work has been done by neurosurgeons in Germany and Japan taking advantage of ALA induced PpIX fluorescence or fluorescein fluorescence guided resection (FGR) of brain tumors. In general, there are three major technological fronts using fluorescence for brain tumor imaging, which can be separated into studies that use:

1. Endogenous autofluorescence;

2. Exogenous agents that are in routine human use (e.g., ALA-PpIX, fluorescein, indocyanine green);
3. Exogenous agents developed as first-time use in humans, with molecular targeting potential.

In the use of these fluorescence biochemical probes, tumors have been visualized using different types of technologies as well, including:

1. In vivo fluorescence microscopy;
2. point spectroscopic tools for imaging one region at a time;
3. modified surgical microscopes or laboratory grade stand-alone systems;
4. commercial systems with built in fluorescence channels;
5. combination systems which integrate fluorescence with spatial imaging;

Recently, the major multicenter clinical efforts have used fluorescence characteristics of brain tumors stimulated through the ALA-PpIX system. Each of these biochemical and technological approaches is discussed in this review. Unfortunately, the different biochemical approaches are intermingled with the different technological approaches, so in this review we focus more on the biochemical choices, and outline the technology used in each case, where appropriate. At the end, we comment on the different technologies used, and how they may be adopted

II. BIOCHEMICAL IMAGING AGENTS

1) Endogenous Fluorescence

Endogenous fluorescence signals from tissue have been extensively studied for brain tumor demarcation and surgical guidance. With this approach, the patient would not require administration of any exogenous drug avoiding medical complications (e.g., allergic reactions, increased liver function tests, etc.), and the procedure is easily implemented. Nonetheless, this approach is still in a pilot study analysis phase. Endogenous autofluorescence still require postoperative data analysis, slightly longer acquisition times (e.g., 30 seconds), and systems are not mainstreamed for real-time neurosurgical applications.

Measurement of endogenous fluorescence signals to assess tissue dysfunction was developed in the late 1980's and early 1990's with the advent of accessible ultraviolet lasers and fibers to sample tissue. Dozens of papers examined the potential in cardiac applications, endoscopy [2] and gynecology [3], using blue and UV light excitation and looking at emission spectra in the blue-green wavelengths. These signals are largely attributed to collagen, NADH, and FAD [4], although identification of the causative nature of the spectra in these layered tissues was a subject of ongoing studies for a decade beyond their initial identification [5] [6]. The confounding effects of tissue layers, light scatter and blood absorption combine to make the spectra harder to interpret. The application of fluorescence measurement in the study of glioma tumors was interestingly predated by most of the exogenous dye studies (as discussed in Section 2.3). In vitro pilot measurements with time-resolved fluorescence showed similar values [7] to that with fluorescence spectroscopy.

Perhaps the most complete in vivo study included both autofluorescence spectral information and white light diffuse reflectance spectroscopy for characterization of tumors [8–9]. In this pilot study on 26 patients, a fiber probe was used intraoperatively. Sequential acquisition of background, fluorescence emission at 337 nm excitation, and diffuse reflectance spectra was followed by biopsy of sampled sites. Discrimination algorithms were

used to distinguish infiltrating tumor margins from normal brain tissue with 100% sensitivity and 76% specificity [8]. In a subsequent study on 24 patients with low and high grade gliomas, they reported sensitivities and specificities of 80% and 89% for differentiating solid tumor from normal tissue, and 94% and 93% for infiltrating tumor margins from normal tissue. This system took approximately 30 seconds to acquire data, with processing done postoperatively. The authors predict that future versions will take less time for acquisition (<5 seconds) and provide real-time feedback for intraoperative guidance [9]. Similar to the work done by the Marcu group, this study took into consideration other optical properties in addition to autofluorescence spectral differences to develop a real-time system for delineation of brain tumor margins and neurosurgical guidance.

2) Protoporphyrin IX

The Aminolevulinic Acid (ALA) – Protoporphyrin IX (PpIX) system has been studied extensively for applications in photodynamic therapy (PDT) and photodiagnosis as well as other fluorescence imaging applications [10–11] including fluorescence-guided resection (FGR) of brain tumors. Administration of ALA overloads the heme synthesis pathway, which exists in all mammalian cells, and fluorescently detectable levels of PpIX are produced in varying degrees [10,12–13]. It is generally the case that the tumor tissue produces higher levels of PpIX than the surrounding normal tissue and a significant difference in PpIX production has been found in brain tumor tissues over normal brain [14–17]. However, different preclinical brain tumor models have been studied and found to have varied PpIX accumulation patterns, making some models more useful for study than others [18].

Interest in ALA-PpIX production for applications in oncology has significantly increased over the past thirty years, with a seminal review paper on this subject published in 1996 by Kennedy, *et al* [11]. ALA-induced PpIX has been extensively investigated as a photosensitizer for PDT in the treatment of many types of cancer. ALA-induced PpIX has found widespread use in dermatology to treat various malignant and non-malignant skin conditions [19–20]. ALA-induced PpIX PDT treatment has been found to be most successful for cancers of hollow organs where the cancerous cells proliferate on the wall of the organ, as opposed to tumors that grow in solid masses, mainly because of the ease of use in topical applications and also because of the high specificity which can be observed in abnormal squamous tissues. PpIX based PDT for bladder carcinoma, Barrett's esophagus, colon carcinoma as well as others have been investigated [13,21].

Due in large part to its success as a tumor margin demarcation tool in neurosurgical resection of human gliomas, a large body of research on ALA-induced PpIX fluorescence of brain tumor cells and tissue currently exists. Conventional therapy for malignant glioma involves surgical resection, fractionated radiotherapy and adjuvant chemotherapy to eradicate the tumor tissue which may remain following attempted surgical resection [22–23]. The infiltrative nature of glioma tumors make them very difficult to fully resect. However, survival following treatment is linked to completeness of tumor removal [24].

Use of the ALA-PpIX system has been very successful for surgical guidance of brain tumor resection [16–17]. Preclinical rabbit models were used to test PpIX fluorescence for surgical guidance of brain tumor resection and found to increase the completeness of tumor resection by a factor of 1.4 and decrease the amount of residual tumor by a factor of 16 from the initial tumor volume [14]. Significant success was also seen in the clinic using ALA-PpIX for fluorescence-guided surgery of malignant glioma resection [16]. In a randomized Phase III multicenter clinical trial using ALA-induced PpIX fluorescence as the tumor tissue contrast agent for neurosurgical guidance, tumor tissue was more completely resected and 6-month progression free survival was extended [17].

A. PpIX Biochemical Production Mechanisms—ALA is a prodrug that is converted to PpIX via the heme synthesis pathway (Fig. 1). Low levels of PpIX exist normally in cells prior to its conversion to heme; however, the pathway can be overloaded with exogenous ALA to produce fluorescently detectable levels of PpIX [11,13,21,25]. PpIX production from ALA is widely variable and it has been shown to be dependent on many factors including ALA uptake and PpIX excretion, morphological features of the cells and tissues as well as the cell microenvironment.

The cause of excess PpIX production in neoplastic cells endogenously and after exogenous ALA administration is much debated. The rate-limiting enzyme in the heme synthesis pathway is ALA synthase, which catalyzes the reaction between glycine and succinyl-CoA to produce endogenous ALA. ALA synthase is subject to feedback inhibition by the build-up of heme in the system and thus ALA is produced only when heme levels are low; however, the addition of exogenous ALA bypasses this enzyme and thus the rate-limiting step. A large body of research on this topic is compiled in a review by Collaud, *et al* [12]. Although much of past research points to porphobilinogen deaminase (PBGD) as the rate limiting enzyme in the ALA-PpIX pathway [13,26], recent research suggests that PBGD may play a minor role in the accumulation of PpIX *in vitro* [27–29]. Additionally, it has been suggested that ALA-dehydratase, which converts ALA to porphobilinogen, may act as the rate-limiting step as its inhibition causes decreased PpIX production [30]. Moreover, the ferrochelatase enzyme that catalyzes the insertion of iron to convert PpIX to heme is thought to have decreased activity in neoplastic cells, allowing selective accumulation of PpIX in these cells [13,31]. The importance of PpIX conversion to heme can also be demonstrated via the use of iron chelators, which increase PpIX production when administered to cells *in vitro* [32–33]. Still other studies suggest that coproporphyrinogen oxidase may be a rate limiting enzyme [34].

B. PpIX Production Variability—The relationships between ALA uptake, PpIX efflux, cellular microenvironment and PpIX cellular content are both complicated and highly variable between cell lines. Studies using exogenously administered radio-carbon labeled ALA demonstrated that the mechanism of uptake was through passive diffusion [35]. Other studies suggested that there may be two mechanisms by which ALA is transported into the cells. Passive diffusion is important at short ALA incubation time intervals, while active transport systems may be more important at longer incubation intervals [36–37]. It was found that both neoplastic and non-neoplastic cells had significantly reduced intracellular PpIX concentrations when incubated in media containing serum, as compared to serum free media, suggesting that the extracellular environment can also play a role in PpIX production [38]. Many environmental factors have also been found to affect PpIX production *in vitro* and are summarized in Table 1.

Cellular mitochondrial contents have also been studied in conjunction with PpIX production. Gibson, *et al* demonstrated that varied PpIX production following administration of ALA was correlated to the number of mitochondria in each cell lines [31]. Liang, *et al* used fluorescence microscopy to examine the subcellular localization of ALA induced PpIX and found that the resulting fluorescence was localized in the mitochondria-rich perinuclear cytoplasm [39]. Additionally, cell size has been found to have a slight positive correlation to PpIX production [40]. In a study completed by Gibbs *et al*, it was found that endogenous PpIX production was positively correlated with mitochondrial content and exogenous PpIX with cell size but not mitochondrial content [41].

C. PpIX Production Enhancement—Two main strategies have been developed to increase ALA-induced PpIX production by altering enzymatic function in the heme synthesis pathway: differentiation therapy and iron chelation [34,42–44]. Differentiation

therapies (including methotrexate, retinoic acid and vitamin D) have been shown to increase PpIX accumulation in prostate cancer cells and keratinocytes [34,43,45–46]. Differentiation therapy was shown to increase cellular PpIX production as well as reduce the fraction of cells that contained low PpIX levels [45]. A possible explanation for this is an increase in the enzyme coproporphyrinogen oxidase at the mRNA and protein levels [34,43]. In contrast, the apparent concentration of PpIX can be increased using iron chelators. In this scenario the availability of iron is diminished, reducing the activity of ferrochelatase and subsequently decreasing the conversion of PpIX to heme. Various iron chelators have been investigated including CP94 (1,2-diethyl-3-hydroxypyridin-4-one hydrochloride), L1 (1,2-dimethyl-3-hydroxy-4-pyridone) desferrioxamine [33,41–42,47]. These iron chelators have been shown to successfully sequester iron from ferrochelatase and increase apparent PpIX levels. Specifically, the use of L1 was tested in a series of neoplastic cell lines, and it was found that iron chelation had the most profound effect on cells that naturally produced low levels of PpIX [41]. Additionally, CP94 is currently in clinical trial to increase PpIX content of basal cell carcinoma for PDT. It was shown that enhancements in tumor reduction were observed when patients received both ALA and CP94 [44]; thus, iron chelation and cellular differentiation appear to be viable methods to increase PpIX production without increasing administered ALA dose.

III. EXOGENOUS CONTRAST AGENTS

For maximal success in brain tumor imaging an exogenous fluorescent molecule or probe should have the following properties: 1) be selective for and retained in the tumor while rapidly cleared from normal tissue or filtered by the BBB; 2) the emission wavelength has a high quantum yield within the tissue (low absorption and scatter from tissue); 3) minimal photobleaching; and 4) does not cause adverse toxicity or phototoxicity effects systemically or locally within the tissue of interest [53]. This section will provide an overview of fluorescence molecules currently used in both animal and human brain tumor imaging (diagnosis, therapeutic monitoring, etc.) and guidance of surgical resection.

1) Organic Fluorescence Molecules

Small, organic molecules that are fluorescent in either the visible or near infrared (NIR) regions of the electromagnetic spectrum make good candidates for tumor visualization. Breakdown of the blood-brain barrier (BBB) is mainly responsible for the delivery of these small exogenous molecules to brain tumors. The molecules are retained within tumor tissue as a result of slow clearance caused by an increase in blood flow and leakage, and a decrease in lymphatic drainage, i.e., the enhanced permeability and retention (EPR) effect. The EPR effect is responsible for increased delivery to tumors of agents administered by intravenous injection and is often exploited, especially in the case of brain tumors [54].

A. Fluorescein Sodium—Fluorescein sodium has been extensively used for FGR of human brain tumors. Fluorescein sodium is a small organic molecular salt (MW 376) with an excitation maximum of 494 nm, an emission maximum of 521 nm at a pH of 8, and a urine clearance of 24–32 hours when injected intravenously. Fluorescein sodium was first reported as a tool for surgical resection of brain tumors in 1948 by Moore [1]; and has regained popularity in the past several decades. The most recent reports have used the technique of Moore, by simply monitoring a combination of the fluorescein sodium staining and fluorescence (appearing as a combination of yellow-green color) of the brain tumor under white light [1,55–59]. This technique is advantageous because it is safe, easy to perform, can be utilized in a dimly lit operating room, and there is no need for extra surgical equipment. In 1998, Kuroiwa et al. developed an intraoperative microscope that enhanced both the observed fluorescence intensity and the normal-to-tumor contrast; allowing more

precise delineation of tumor margins [60]. However, this intraoperative microscopy is not readily used today because it requires excess equipment and surgical maneuvering. One thing to note is that fluorescein can have deleterious side effects, especially if injected quickly or in a very high concentration [61].

B. Indocyanine Green—Indocyanine green (ICG), or Cardio-Green, is a small water soluble organic molecule (MW 744 g/mol) commonly used in angiography as well as to probe cardiac and liver function. The Berger group demonstrated ICG staining of tumor tissue using an orthotopic rat glioma model [62]. It was shown that the observed colored demarcation caused by ICG staining of the tumor tissue coincided within 1 mm of the histological tumor margins. However, these results were obtained with ICG doses exceeding the LD-50 for rats. It was later shown that lower doses of ICG could be used in both rats and humans with the implementation of enhanced optical imaging: a technique of subtracting reflectance images pre- and post-ICG administration to enhance staining visibility [63–64]. More recently, the bradykinin analog RMP-7 has been used to increase the permeability of the tumor vasculature prior to ICG administration, thus maximizing the EPR effect and effectively increasing the amount of ICG delivered to the tumor tissue [65]. It should be noted that the tissue staining in these cases do not require the use of the ICG fluorescence properties, but simply the color staining of the tissue. However, the NIR properties of ICG fluorescence emission would make this a good candidate for fluorescence-guided surgical resections.

IV. NANOPARTICLES

The term nanoparticle broadly describes any organic or inorganic material-based particle of nanometer size, and generally unique properties of the particle arise due to size restrictions. In general, nanoparticles can be functionalized and used in a multimodality function for a variety of imaging techniques (optical, MRI, etc.), tissue targeting, drug therapy, and size distribution. This section investigates the most common types of nanoparticles used in brain tumor imaging, while the next section will cover functionalization for delivery and tissue targeting.

Quantum Dots

Quantum dots (QDs) are nanoparticles constructed from semiconducting nanocrystals and have several advantageous optical properties [66–67]. The emission wavelength is tunable based on the diameter of the nanocrystal and displays very bright, stable fluorescence. The emission bandwidth is very narrow while the excitation bands are broad allowing excitation with a wide variety of laser and light sources. QDs are generally hydrophobic and therefore require a wide variety of surface functionalization in order to render them soluble in biologically relevant solvents, e.g. polyethylene glycol (PEG), lipids, and dextrans [68]. These surface modifications are not used for targeting but have added benefit for passive targeting. Unless the QD is specifically labeled for targeting, the general mechanism for entry into a cell is through phagocytosis by the reticuloendothelial system – specifically through monocytes or macrophages [68]. Within the last several years there have been many examples of quantum dots used for the determination of tumor boundaries using both passive [68–69] and targeted delivery methods.[70–72]. Although QDs provide very high contrast and tumor localization, the largest drawback to their use is that the long term effects of QD administration are generally unknown and strongly debated as clearance from both tissue and body is an important factor in toxicity [73]. In 2007, Choi et al demonstrated that QDs with a hydrodynamic radii less than 5.5 nm were rapidly cleared by the renal system, meanwhile functionalized QDs with hydrodynamic radii larger than 5.5 nm were not [74].

These results suggest care should be taken in the long term effects of QDs retained within the body.

Polymer Based Nanoparticles

Polyamidoamine dendrimers are nanoparticles consisting of many branched polymer chains that can be functionalized with imaging, targeted delivery, and therapeutic agents [75]. Sarin et al (2008) functionalized these dendrimer nanoparticles with rhodamine B and gadolinium such that in vivo MR imaging and ex vivo fluorescence imaging could be performed on rats [75]. Although this experiment was performed to test the BBB size exclusion limit (discussed further in the *Passive Targeting section*), these nanoparticles could easily be functionalized for diagnostic or surgical based fluorescence detection. Polyacrylamide nanoparticles can be loaded with a variety of organic dyes or inorganic materials and functionalized for targeted delivery [76]. Recently, Orringer et al demonstrated that these nanoparticles could be loaded with a variety of small organic molecules (methylene blue, Coomassie blue, or indocyanine green) to cause a color change in the brain tumor tissue, while reducing the cytotoxic effects of these molecules [76]. Although the fluorescent properties of these molecules were not utilized, it can be imagined that this could be easily implemented.

Iron Oxide Nanoparticles

Iron oxide nanoparticles below 30 nm in diameter are superparamagnetic and have been extensively used in tumor targeting, both for imaging and therapy [77]. In a standard MRI T2 imaging sequence, the superparamagnetic iron oxide nanoparticles provide negative contrast, while simultaneously being used as a therapeutic or targeting agent.[78] Nanoparticles 10 – 100 nm in diameter are too large to undergo renal elimination and as such have long blood half-lives [79]. Functionalization can be performed to produce nanoparticles with passive targeting abilities (reticuloendothelial cell mediated phagocytosis), active targeting abilities (ligand-receptor mediated or other biomarkers) and fluorescence properties for optical imaging [80]. CLIO-Cy5.5 is an iron oxide nanoparticle has been developed as a pre-operative MR imaging agent and an intraoperative fluorescence probe [79,81]. CLIO-Cy5.5 is coated in cross-linked dextran and then covalently linked to Cy5.5 [79]. It has been found that the CLIO-Cy5.5 marker provides accurate demarcation of the tumor margin and a strong co-localization of MR images and intraoperative fluorescence since both signals are produced from the same particle [79,81]. Another similar particle has been reported in which iron oxide nanoparticles are coated in polyethylene glycol (PEG) and then covalently linked to Cy5.5 for optical imaging and chlorotoxin for cellular targeting [82–84].

V. DELIVERY METHODS

The BBB prohibits the infiltration of most foreign and endogenous small molecules into the brain; However, a compromised BBB in some brain tumors provides most of the apparent contrast to tumor tissues that can be distinguished radiologically or through fluorescence contrast. Most of the work described here has been in the area of passive delivery via this mechanism, whereas targeted delivery to brain tumors is the area which will likely provide delineation of micro-invasive disease, and radiologically occult lesions [85].

Passive Targeting

Sain et al used gadolinium and rhodamine B multi-functionalized dendrimers to test the size exclusion of RG-2 malignant gliomas [75]. They found that functionalized nanoparticles less than 11.9 nm could pass through the BBB of a glioma model, whereas larger particles could

not. The size exclusion of the BBB would depend on the extent of BBB breakdown and would most likely progress with tumor infiltration and progression.

Serum albumin makes up 50–70% of the human plasma protein reserve and it has been well documented that tumor tissues use serum albumin as a source of amino acids and energy [86–88]. Small organic molecules can rapidly bind to serum albumin and other plasma proteins with increased distribution and retention occurring if molecules are labeled prior to administration [62]. In 2000, Kemeret al demonstrated the feasibility of using 5-aminofluorescein linked to serum albumin as a fluorescent tumor cell marker by intravenously injecting a C6-glioma [89]. Twenty-four hours after administration of drug, the fluorescence within the tumor was 23-fold higher than that of normal brain tissue with tumor borders sharply demarcated. Successful human clinical trials were performed in both 2000 and 2009 using this system [53,89].

Active targeting

Epidermal growth factor (EGF) and the EGF receptor (EGFR) are known to be upregulated in many types of cancers and correlated with tumor growth and aggressiveness [90]. Small organic molecules and nanoparticles can be conjugated to EGFR-targeting agents to increase both retention of fluorescent molecules and contrast observed between tumor and normal tissue. The two most common ways to target EGFR is by either directly labeling EGF, or labeling an anti-EGFR monoclonal antibody (e.g., C225, Erbitux, cetuximab). Extensive work has been performed with the commercially available EGF conjugated IRDye 800CW (EGF-IRDye) from LI-COR Biosciences (Lincoln, NE) [91–92]. This dye has been administered to mice bearing one of three tumor lines (9L-GFP, U251, and U251-GFP), and monitored using a variety of in vivo and ex vivo imaging techniques for tumor diagnostics and boundary delineation (Figure 2) [91–92]. Of particular interest, tumors which were not apparent by contrast MR imaging (U251-GFP) could be detected optically with the EGF-IRDye adding diagnostic value [91]. Wang et al coated QDs with anti-EGFR antibodies and found that the targeted QDs localized selectively in tumors expressing EGFR within 30 minutes of intravenous administration [71]. Additionally, Arndt-Jovin et al demonstrated that clear demarcation between normal brain and tumor tissue could be observed with QDs labeled with either EGF or anti-EGFR (Her1) in cell culture, mouse models and human brain-tumor biopsy sections [70]. Although there is advantageous targeting with EGF-bound fluorophores, it must be noted that this only occurs with tumors overexpressing EGF and EGFR. Tumors that have no or low expression of EGFR do not display enhanced contrast when targeted agents such as EGFR targeted probes are administered [71]. This can reflect the specific biology of the tumor, where some high grade gliomas (e.g., glioblastoma multiforme) may have high levels of EGF and EGFR, while many low grade gliomas tend to have minimal levels of the growth factor and receptor [90].

Enzyme Function targeting

A successful example of enzymatic function targeting is ProSense, a molecular probe that monitors the protease activity in diseased tissues. The intravenously injected probe molecule consists of a polylysine backbone with quenched NIR fluorophores that becomes activated upon cleavage by disease-associated cathepsins, first reported by Weissleder et al. in 1999 [93]. ProSense is now commercially available from VisEn Medical (Bradford, MA, USA) in a 680 nm form (excitation $680\pm 10\text{nm}$, emission $700\pm 10\text{nm}$) and a 750 nm form (excitation $750\pm 10\text{nm}$, emission $780\pm 10\text{nm}$) as well as in non-cleavable controls. Recently, McCann et al reported the use of ProSense 680 activated NIR fluorescence probe for the application of fluorescence molecular tomography (FMT) combined with magnetic resonance imaging (MRI) [94]. It was shown that tumor volume increases observed with MRI after

chemotherapy correlated with underlying histological changes reported by the activated ProSense fluorescence signal.

Peptide targeting

Conjugation of small peptides to the surface of nanoparticles is proposed as a promising targeting approach, more so than antibodies or larger proteins, due to the polyvalent interactions that can be achieved between the numerous ligands and receptors on the cell surface [95]. Cai et al (2006) demonstrated that QDs labeled with a three residue peptide arginine-glycine-aspartic acid (RGD) could target tumor vasculature, specifically binding to integrin $\alpha_v\beta_3$, in a U87MG human glioblastoma mouse model [72]. In fact, the QD705-RGD nanoparticle gave better tumor to normal tissue contrast than a Cy5.5-RGD conjugated tested in 2004 by the same group [96]. However, due to its much smaller size Cy5.5-RGD had much faster localization times and was able to bind to integrins on both vascular and cell surfaces, while the QD705-RGD only bound to vascular surfaces [72,96]. Another interesting use of peptide labeled nanoparticles has been reported from the Zhang group, where a 36 amino acid chlorotoxin peptide and AlexaFluor 680 were used to label multifunctional iron oxide nanoparticle coated in PEG silane [82–84]. Chlorotoxin has both targeting and therapeutic value as an inhibitor of cell invasion [82]. This multifunctional nanoparticle provides a modality for cellular targeting (chlorotoxin), MR imaging (iron oxide core), FGR (AF680), and potential therapeutic value (chlorotoxin).

VI. INSTRUMENTATION

1) Microscopy In Vivo

Many developments have occurred in the past few decades to bring microscopy to in vivo use. In vivo confocal fluorescence microscopy is now commonly available and routinely used for research applications. Clinical use of microscopy has been largely limited to research trials, where mechanistic information is sought about the origins of uptake or localization [97]. Multiphoton microscopy of the localization and generation of PpIX was examined [98], with good indication that the approach might provide information on localization, as needed. Now, commercially available in vivo confocal microscopes are available, and while in principle the use of these could expand, the utility may be limited by the small field of view inherent in microscopy.

2) Fiber Probe Systems

Imaging fiber probes have been demonstrated for several decades now [99], with endoscopy type imaging systems now being the standard approach [100]. Although neurosurgical applications tend to focus around the non-contact surgical microscopy instruments that are standard in surgical resection today, the desire for maximum information drives the desire for point sampling probes which provide better wavelength spectroscopy and usually higher overall sensitivity due to the maximal capture of light [101]. The design of the fiber probe clearly affects the depth of sampling [102], the tissue sampling volume [103], and the spatial resolution to which the surgeon can use the information. While early designs have not focused on these issues all that effectively, later developments have focused on making sure the utility matches the clinical need [102]. Several designs have focused around the need for quantitative information and reducing the size to less than one scattering distance has been one successful approach [104], while others focus on using a ratio of different wavelengths to remove background tissue effects [105–106].

Much of the *in vivo* spectroscopy of PpIX in brain tumors has been accomplished in Japan [107–109]. Ishihara et. al. examined surgical biopsy specimens from six histologically confirmed diffusely infiltrating astrocytomas [107] by studying the fluorescence intensity

ratios of the PpIX peak at 635 nm to the peak emission intensity of the reflected excitation light. They correlated the intensity ratios to various histological parameters, such as proliferation, microvessel density and vascular endothelial growth. The authors found a strong correlation between tumor proliferation and fluorescence intensity ratios ($R = 0.929$, $p < 0.001$). Further work by Utsuki et. al. examined six patients that did not exhibit macroscopic intraoperative PpIX fluorescence, and found that areas with an amplitude peak at 636 nm contained diffuse astrocytoma tumor cells [109]. This group developed an auditory alert system, where the surgeon would be alerted when the difference in relative intensity between 636 nm and 632 nm was greater than 500, and used it on six patients with glioblastoma [108]. Using this, all samples with visible macroscopic fluorescence were accurately detected, and three areas without macroscopic fluorescence were found, which were subsequently confirmed as infiltrating tumor regions. This increase in sensitivity to areas which cannot be effectively imaged is the attraction of using some higher sensitivity probe system in vivo or in situ.

A high resolution, non-contact, multispectral fluorescence imaging system was studied that could detect red Photofrin® fluorescence at the tissue surface or up to a 0.5 mm depth [110]. This study was part of a phase III clinical trial using PDT following radical resection of GBM. In that study it was possible to determine minimal levels of Photofrin® fluorescence intraoperatively in tissues followed by histologic confirmation. The advantage of the system was high sensitivity for fluorophore levels and that multispectral capability will allow for easy adaptation to other fluorophores, e.g., PpIX and fluorescein.

Although the intraoperative spectroscopic analysis of brain tissues for quantification and qualification of minimal PpIX fluorescence has yet to be clinically accepted, there are advantages over current FGR techniques. With macroscopic fluorescence, the neurosurgeon is capable of resecting the bulk of tumor tissue, but margins with diffusely infiltrating tumor cells are left with less certainty. It is in these diffusely infiltrating areas that intraoperative PpIX spectroscopy should provide neurosurgical guidance for highly sensitive and specific detection of diffusely infiltrating tumor margins.

3) Modified Clinical Surgical Microscope

The first report using intra-operative fluorescence guidance system was demonstrated in 1948 by Moore et. al., where forty-six patients with brain tumors were administered fluorescein sodium and treated under guidance of a yellow-green fluorescence without the use of a modified surgical microscope [55,61]. In a similar fashion, in 1982 Murray reported on an experience on 23 patients with grade II, III, and IV astrocytomas, 3 lymphomas, and 3 metastatic cancers [55], and noted that 84.7% of tissues that displayed macroscopic, visible fluorescence under white light illumination were positive for neoplasia and the other 15.3% were necrotic tissue. These two initial experiences using fluorescein for FGR proved to be of value for neurosurgeons in visually identifying neoplastic tissues with an abnormally permeable blood-brain barrier.

Further work has been carried on in Japan [57–58,60,111], Turkey [56], and Germany [53,89] using fluorescein for FGR of malignant gliomas and metastatic brain tumors. Kuroiwa et. al. developed a modified fluorescein operative microscope with a BP 450–490 nm excitation filter and a Kodak Wratten No. 12 filter to capture the peak emission at 500–530 nm [60]. Fluorescein sodium was administered intravenously with a wait time of 20 minutes from the moment of injection to the start of resection. The authors treated 10 patients with a diagnosis of high grade glioma and achieved a high rate of complete resection confirmed by postoperative MRI. This initial report showed the utility of this modified fluorescein operative microscope for FGR and intraoperative determination of tumor margins. Additional studies confirmed the value in malignant glioma resection [111].

They once again noted the usefulness of fluorescein for FGR in cases with radiological contrast enhancement on CT and MRI.

With the discovery of the ALA-PpIX contrast mechanism, Stummer et. al. [112] used a modified surgical microscope with a xenon light source that could switch intraoperatively from the standard white light to the excitation violet-blue light mode (375–440 nm). PpIX fluorescence with peaks at 635 and 704 nm were viewed using a 455 nm long pass filter. This microscope was used in a few modified forms to carry out their institutional trial, and a production scale system was developed by Leica for the Phase III studies.

More recently tunable filters have been used for imaging fluorescence, allowing flexibility in choosing wavelengths for excitation and emission[113]. Systems which integrate intelligent algorithms for multispectral imaging are being developed and evaluated in trials, and will likely take some significant role in the optimal design of a clinical prototype [114]. Figure 3 shows white light and fluorescence imaging during high grade glioma tumor resection in a subject in the ongoing Dartmouth trial, using the current version of the Zeiss system. The commercial systems available today are produced by Leica, Zeiss, and Olympus, which are either specifically designed for fluorescence neurosurgery applications, or could be used in this capacity for investigator initiated research trials.

4) Image-Guided Systems

The realm of image-guidance during neurosurgery has matured significantly in recent years. Systems that include pre-operative MR or CT images can be merged with fluorescence microscopy and research into this integration is ongoing. The ability to integrate fluorescence tomography with CT and MRI has been demonstrated in pre-clinical work[91], for brain lesion imaging. This type of specialized instrumentation can be extended to human use, through the creation of customized interfaces[115]. Optical probes that enhance the visualization of pre-operative imaging and are co-localized with intraoperative fluorescence imaging are all part of the toolbox that will allow accurate image-guidance, once proven clinically viable [79]. Integration of pre-operative imaging with intra-operative imaging which provide real time imaging of the brain structure and with fluorescence guidance overlays would be the ideal goal, and such systems are under research development.

VII. CLINICAL TRIALS & CONSENSUS STUDIES

The rationale for this work is obvious from the bleak evidence of moderately high incidence with a low survival rate of brain tumors [116]. Malignant gliomas account for approximately 70% of new cases of malignant primary brain tumors in the United States [117]. Malignant gliomas are histologically heterogeneous and infiltrating tumors of glial precursor cells that can be divided into two major categories: astrocytomas and oligodendrogliomas [116–118]. These tumors are graded on a scale of I to IV based on several histological parameters, e.g., nuclear atypia, mitotic figures, necrosis, etc., which are essential for guidance of treatment and patient prognosis [116–118]. Glioblastoma multiforme (GBM) is a grade IV glial tumor that accounts for approximately 60–70% of malignant gliomas, with a 5-year survival rate of 3.3% and median survival of 1 year. This is compared to 5-year survival rates greater than 70% for lower grade gliomas [116–117,119]. One other important common class of intracranial neoplasms are meningiomas, accounting for 20% of intracranial neoplasms [116]. It is important to note that different brain tumors require different treatment options, with the degree of resection an important prognostic factor in glioblastomas and meningiomas [17,116,120–125]

With this complex array of tumor types and wide variation in successful response to therapy, the need for better customized tools is compelling.

1) ALA-PpIX Imaging Consensus Studies

Over the last decade, the largest clinical effort with ALA-PpIX was in Germany. Stummer et. al. [112] reported using FGR on ten patients with malignant gliomas showed that tissue fluorescence had an 85% sensitivity and 100% specificity of predicting the presence of malignancy in tissue biopsies and was confirmed by spectroscopic analysis. In this study, fluorescence was useful in defining regions with the presence of tumor for high grade gliomas, but not for low grade gliomas [112]. These promising results led the German team to perform a prospective study evaluating the influence of FGR on post-operative MRI and patient survival [16]. Sixty-six patients were treated and 52 with a diagnosis of glioblastoma multiforme were included in the final analysis. This prospective trial showed a strong relationship between residual intraoperative fluorescence and residual contrast enhancement (CE) on MRI ($\chi^2 = 10.2$, $p = 0.0014$) and led the authors to conclude that observed survival was significantly dependent on the residual CE on MRI and residual fluorescence. In addition, this study prompted a randomized controlled trial.

The ALA-Glioma Study Group in Germany led a large, randomized controlled, multicenter phase III clinical trial to assess the influence of FGR using ALA induced PpIX fluorescence on extent of surgical resection, progression free survival, morbidity, and overall survival [17]. Patients were randomly assigned to FGR using ALA or standard white light guided resection (WGR), where the primary endpoints of the study were the number of patients without postoperative CE tumor and 6-month progression free survival. An analysis on 270 patients showed: 1) complete removal of CE tumor was more frequent in patients undergoing FGR vs WGR (65% vs 36%); 2) progression free survival, i.e., absence of radiological progression of disease at six months, was higher in patients undergoing FGR vs WGR (41% vs 21%); 3) there was no difference in frequency of adverse effects between the two groups. Furthermore, it showed that patients with complete tumor resection, i.e., absence of residual CE on postoperative MRI, had a higher overall median survival than those with residual CE on postoperative MRI (17.9 months vs 12.9 months, $p < 0.0001$). Subsequent analysis of the data from this phase III trial was performed to adjust for factors that would influence the degree of resection [124]. One major difference between the complete resection (CR) and the incomplete resection groups (IR) was age; more patients in the CR group were younger than the median of 60 years. In the initial analysis the median survival was greater in the CR than in the IR group (16.7 vs 11.8 months, $p < 0.0001$) and after adjustment for age, a significant difference between CR and IR was still observed independent of age.

The ALA-Glioma Study Group performed a final reanalysis of the data from the phase III trial using the Radiation Therapy Oncology Group-Recursive Partitioning Analysis (RTOG-RPA) criteria to assess whether there was a benefit from extensive resection of tumor [123]. Patients were stratified by resection status (CR vs IR) within RTOG-RPA classes III, IV, V. This analysis showed that patients undergoing CR had a higher survival in the prognostically unfavorable RTOG-RPA classes IV and V than those undergoing IR. The repartitioning of the ALA-Glioma Study group phase III trial once again showed the significance of CR in treatment of glioblastoma with an increase in survival

There have been several studies in Japan for the treatment of glioblastomas, anaplastic astrocytomas, and meningiomas [100,126–131]. Additionally, a one year experience in Switzerland with 74 patients [132], and an ongoing clinical trial at Dartmouth Hitchcock Medical Center have made use of this technology [133–134]. The work in Japan has shed light on the applications and limitations of ALA induced PpIX fluorescence in FGR. Utsuki et. al, performed a histological examination on patients that underwent FGR of glioblastoma or metastatic brain tumors. They reported false positives in malignant gliomas as well as in metastatic brain tumors due to histological signs of neutrophil infiltration, reactive

astrocytosis, or macrophage infiltration [127]. Another report by Utsuki et. al. described an experience with 11 cases of metastatic brain tumors, of which nine showed PpIX fluorescence. Thirty-one fluorescent samples from the tumor bulk showed the presence of tumor cells, and 25 out of 27 samples with vague fluorescence from the peritumoral area showed edematous brain tissue without tumor cells [127]. In another experience on patients with non-neoplastic lesions the investigators reported PpIX fluorescence in areas of positive contrast enhancement on MRI that were histologically verified as radiation necrosis and demyelinating disease [135]. Another report also presented a fluorescence guided endoscopic procedure for the detection of a deeply seated anaplastic astrocytoma displaying strong fluorescence [100]. In addition to providing multiple other uses for PpIX fluorescence in brain disease, these reports highlighted limitations in the lack of tumor specificity of PpIX fluorescence. Nevertheless, these reports provide evidence that PpIX fluorescence localizes to abnormal tissue, whether it is tumor, necrotic, or demyelinating brain tissue. This knowledge should inform surgeons and be kept in mind when using currently accepted treatments (e.g., FGR for treatment of glioblastomas) or when developing new applications.

Major contributions for the use of ALA induced PpIX fluorescence in FGR of meningiomas have been made by research groups in Japan [129,131]. In a series of 24 patients with meningioma the PpIX fluorescence sensitivity and specificity for the main tumor were 83% and 100%, respectively. Furthermore, PpIX fluorescence sensitivity and specificity for hypertrophic, non-tumorous dura was 100% and 83%, respectively [131]. The authors did not find a strict correlation between proliferation and fluorescence nor was there a relationship between degree of malignancy and fluorescence; whereas studies of astrocytomas have shown that proliferation levels were a significant factor for PpIX fluorescence [107,136]. More work remains to further understand the factors that influence PpIX fluorescence in malignant gliomas and meningiomas, but extension of this practical FGR technology has shown promise for maximizing the extent of resection in these tumors [129,131].

A single centre, phase III randomized clinical trial was performed using ALA and Photofrin® for FGR and repetitive photodynamic therapy (PDT) [137]. Twenty-seven patients were recruited; 14 were assigned ALA and Photofrin® FGR followed by repetitive PDT, and 13 were treated with standard neuronavigation and WGR. Survival was significantly increased in the treatment group compared to the control group (52.8 weeks vs 24.6 weeks, $p < 0.01$). The results from this study are promising, but warrant a larger, multicenter randomized controlled trial to further assess the survival advantage of combined ALA induced PpIX fluorescence and Photofrin® FGR-PDT.

VIII. CONCLUSIONS

The systems and biomarkers available are a complicated match up, however neurosurgical guidance of tumor resection is one of the key areas where fluorescence imaging appears to have immediate impact. Part of this is due to the fact that brain tumors have such poor prognosis in general, and any tools to help improve the resection can have immediate short term benefit on patient's lives. However, the brain is a unique organ, where tumor contrast relative to normal brain can be quite high, and fluorescence guidance has benefit, simply as visualized by the surgeon's eye.

A substantial benefit for brain tumor patients will likely come in improved systems to track weak fluorescence signals in areas not well resected using current systems, and in tumor sub-types that do not present well with ALA-PpIX fluorescence or vascular marking fluorescence such as fluorescein or ICG.

Improvements in molecular markers taken up in micro-invasive disease and which allow molecular fingerprinting of tumor will be extremely useful, and promising agents must overcome the financial and regulatory barriers that currently limit their initiation into phase I trials.

Acknowledgments

This work has been funded by NIH grants RO1CA109558 and RO1NS052274.

REFERENCES

1. Moore GE, et al. The clinical use of fluorescein in neurosurgery; the localization of brain tumors. *J Neurosurg* 1948 Jul;vol.5:392–398. [PubMed: 18872412]
2. Richards-Kortum R, et al. Spectroscopic diagnosis of colonic dysplasia. *Photochemistry & Photobiology* 1991 Jun;vol. 53:777–786. [PubMed: 1653427]
3. Ramanujam N, et al. Fluorescence spectroscopy: a diagnostic tool for cervical intraepithelial neoplasia (CIN). *Gynecologic Oncology* 1994 Jan;vol. 52:31–38. [PubMed: 8307499]
4. Georgakoudi I, et al. NAD(P)H and collagen as in vivo quantitative fluorescent biomarkers of epithelial precancerous changes. *Cancer Research* 2002 Feb 1;vol. 62:682–687. [PubMed: 11830520]
5. Croce AC, et al. Diagnostic potential of autofluorescence for an assisted intraoperative delineation of glioblastoma resection margins. *Photochem. Photobiol* 2003;vol. 77:309–318. [PubMed: 12685660]
6. DaCosta RS, et al. Molecular fluorescence excitationemission matrices relevant to tissue spectroscopy. *Photochem. Photobiol* 2003;vol. 78:384–392. [PubMed: 14626667]
7. Yong WH, et al. Distinction of brain tissue, low grade and high grade glioma with time-resolved fluorescence spectroscopy. *Frontiers in Bioscience* 2006;vol. 11:1255–1263. [PubMed: 16368511]
8. Lin WC, et al. In vivo brain tumor demarcation using optical spectroscopy. *Photochemistry & Photobiology* 2001 Apr;vol. 73:396–402. [PubMed: 11332035]
9. Toms SA, et al. Intraoperative optical spectroscopy identifies infiltrating glioma margins with high sensitivity. *Neurosurgery* 2005 Oct;vol. 57:382–391. discussion 382-91. [PubMed: 16234690]
10. Friesen SA, et al. 5-Aminolevulinic acid-based photodynamic detection and therapy of brain tumors (review). *International Journal of Oncology* 2002;vol. 21:577–582. [PubMed: 12168102]
11. Kennedy JC, et al. Photodynamic therapy (PDT) and photodiagnosis (PD) using endogenous photosensitization induced by 5-aminolevulinic acid (ALA): mechanisms and clinical results. *Journal of Clinical Laser Medicine & Surgery* 1996;vol. 14:289–304. [PubMed: 9612195]
12. Collaud S, et al. On the selectivity of 5-aminolevulinic acid-induced protoporphyrin IX formation. *Current Medicinal Chemistry Anti Cancer Agents* 2004;vol. 4:301–316. [PubMed: 15134506]
13. Peng Q, et al. 5-Aminolevulinic acid-based photodynamic therapy. Clinical research and future challenges. *Cancer* 1997;vol. 79:2282–2308. [PubMed: 9191516]
14. Bogaards A, et al. Increased brain tumor resection using fluorescence image guidance in a preclinical model. *Lasers in Surgery & Medicine* 2004;vol. 35:181–190. [PubMed: 15389738]
15. Olivo M, Wilson BC. Mapping ALA-induced PPIX fluorescence in normal brain and brain tumour using confocal fluorescence microscopy. *International Journal of Oncology* 2004;vol. 25:37–45. [PubMed: 15201987]
16. Stummer W, et al. Fluorescence-guided resection of glioblastoma multiforme by using 5-aminolevulinic acid-induced porphyrins: a prospective study in 52 consecutive patients. *J Neurosurg* 2000 Dec;vol. 93:1003–1013. [PubMed: 11117842]
17. Stummer W, et al. Fluorescence-guided surgery with 5-aminolevulinic acid for resection of malignant glioma: a randomised controlled multicentre phase III trial. *Lancet Oncol* 2006 May;vol. 7:392–401. [PubMed: 16648043]
18. Hebeda KM, et al. 5-Aminolevulinic acid induced endogenous porphyrin fluorescence in 9L and C6 brain tumours and in the normal rat brain.[erratum appears in *Acta Neurochir (Wien)*

- 1998;140(8):881]. *Acta Neurochirurgica* 1998;vol. 140:503–512. discussion 512-3. [PubMed: 9728253]
19. Ericson MB, et al. Photodynamic therapy of actinic keratosis at varying fluence rates: assessment of photobleaching, pain and primary clinical outcome. *British Journal of Dermatology* 2004;vol. 151:1204–1212. [PubMed: 15606516]
 20. Gupta AK, Ryder JE. Photodynamic Therapy and Topical Aminolevulinic Acid An Overview. *American Journal of Clinical Dermatology* 2003;vol. 4:699–708. [PubMed: 14507231]
 21. Kelty CJ, et al. The use of 5-aminolaevulinic acid as a photosensitiser in photodynamic therapy and photodiagnosis. *Photochemical & Photobiological Sciences* 2002;vol. 1:158–168. [PubMed: 12659511]
 22. Tam Truong M. Current role of radiation therapy in the management of malignant brain tumors. *Hematology Oncology Clinics of North America* 2006;vol. 20:431–453.
 23. Tuettenberg J, et al. Angiogenesis in malignant glioma-A target for antitumor therapy? *Critical Reviews in Oncology Hematology* 2006;vol. 59:181–193.
 24. Stummer W, et al. Intraoperative detection of malignant gliomas by 5-aminolevulinic acid-induced porphyrin fluorescence. *Neurosurgery* 1998 Mar;vol. 42:518–525. discussion 525-6. [PubMed: 9526986]
 25. Brown SB, et al. The present and future role of photodynamic therapy in cancer treatment. *Lancet Oncology* 2004;vol. 5:497–508. [PubMed: 15288239]
 26. Hinnen P, et al. Biochemical basis of 5-aminolaevulinic acid-induced protoporphyrin IX accumulation: a study in patients with (pre)malignant lesions of the oesophagus. *British Journal of Cancer* 1998;vol. 78:679–682. [PubMed: 9744510]
 27. Hilf R, et al. Effect of delta-aminolevulinic acid on protoporphyrin IX accumulation in tumor cells transfected with plasmids containing porphobilinogen deaminase DNA. *Photochemistry & Photobiology* 1999;vol. 70:334–340. [PubMed: 10483361]
 28. Gibson SL, et al. A regulatory role for porphobilinogen deaminase (PBGD) in delta-aminolaevulinic acid (delta-ALA)-induced photosensitization? *British Journal of Cancer* 1998;vol. 77:235–243. [PubMed: 9460994]
 29. Krieg RC, et al. Cell-type specific protoporphyrin IX metabolism in human bladder cancer in vitro. *Photochemistry & Photobiology* 2000;vol. 72:226–233. [PubMed: 10946577]
 30. Gibson SL, et al. Is delta-aminolevulinic acid dehydratase rate limiting in heme biosynthesis following exposure of cells to delta-aminolevulinic acid? *Photochemistry & Photobiology* 2001;vol. 73:312–317. [PubMed: 11281029]
 31. Gibson SL, et al. Relationship of delta-aminolevulinic acid-induced protoporphyrin IX levels to mitochondrial content in neoplastic cells in vitro. *Biochemical & Biophysical Research Communications* 1999;vol. 265:315–321. [PubMed: 10558864]
 32. Bech O, et al. The pH dependency of protoporphyrin IX formation in cells incubated with 5-aminolevulinic acid. *Cancer Letters* 1997;vol. 113:25–29. [PubMed: 9065797]
 33. Chang SC, et al. The efficacy of an iron chelator (CP94) in increasing cellular protoporphyrin IX following intravesical 5-aminolaevulinic acid administration: an in vivo study. *Journal of Photochemistry & Photobiology. B Biology* 1997;vol. 38:114–122.
 34. Sinha AK, et al. Methotrexate used in combination with aminolaevulinic acid for photodynamic killing of prostate cancer cells. *Br J Cancer* 2006 Aug 21;vol. 95:485–495. [PubMed: 16868543]
 35. Gibson SL, et al. Time-dependent intracellular accumulation of delta-aminolevulinic acid, induction of porphyrin synthesis and subsequent phototoxicity. *Photochemistry & Photobiology* 1997;vol. 65:416–421. [PubMed: 9077122]
 36. Bermudez Moretti M, et al. Delta-Aminolevulinic acid transport in murine mammary adenocarcinoma cells is mediated by beta transporters. *British Journal of Cancer* 2002;vol. 87:471–474. [PubMed: 12177786]
 37. Correa Garcia S, et al. Mechanistic studies on delta-aminolevulinic acid uptake and efflux in a mammary adenocarcinoma cell line. *British Journal of Cancer* 2003;vol. 89:173–177. [PubMed: 12838320]
 38. Wyld L, et al. Factors affecting aminolaevulinic acid-induced generation of protoporphyrin IX. *British Journal of Cancer* 1997;vol. 76:705–712. [PubMed: 9310234]

39. Liang H, et al. Subcellular phototoxicity of 5-aminolaevulinic acid (ALA). *Lasers in Surgery & Medicine* 1998;vol. 22:14–24. [PubMed: 9443145]
40. Moan J, et al. Protoporphyrin IX accumulation in cells treated with 5-aminolevulinic acid: dependence on cell density, cell size and cell cycle. *International Journal of Cancer* 1998;vol. 75:134–139.
41. Gibbs SL, et al. Protoporphyrin IX level correlates with number of mitochondria, but increase in production correlates with tumor cell size. *Photochem Photobiol* 2006 Sep–Oct;vol. 82:1334–1341. [PubMed: 16771607]
42. Berg K, et al. The influence of iron chelators on the accumulation of protoporphyrin IX in 5-aminolaevulinic acid-treated cells. *Br J Cancer* 1996 Sep;vol. 74:688–697. [PubMed: 8795569]
43. Ortel B, et al. Differentiation-specific increase in ALA-induced protoporphyrin IX accumulation in primary mouse keratinocytes. *Br J Cancer* 1998 Jun;vol. 77:1744–1751. [PubMed: 9667642]
44. Pye A, et al. Enhancement of methyl-aminolevulinate photodynamic therapy by iron chelation with CP94: an in vitro investigation and clinical dose-escalating safety study for the treatment of nodular basal cell carcinoma. *J Cancer Res Clin Oncol* 2008 Aug;vol. 134:841–849. [PubMed: 18239941]
45. Ortel B, et al. Differentiation enhances aminolevulinic acid-dependent photodynamic treatment of LNCaP prostate cancer cells. *Br J Cancer* 2002 Nov 18;vol. 87:1321–1327. [PubMed: 12439724]
46. Sato N, et al. Vitamin D enhances ALA-induced protoporphyrin IX production and photodynamic cell death in 3-D organotypic cultures of keratinocytes. *J Invest Dermatol* 2007 Apr;vol. 127:925–934. [PubMed: 17068479]
47. Pourzand C, et al. The iron regulatory protein can determine the effectiveness of 5-aminolevulinic acid in inducing protoporphyrin IX in human primary skin fibroblasts. *J Invest Dermatol* 1999 Apr;vol. 112:419–425. [PubMed: 10201523]
48. Wyld L, et al. Aminolaevulinic acid-induced photodynamic therapy: cellular responses to glucose starvation. *British Journal of Cancer* 2002;vol. 86:1343–1347. [PubMed: 11953896]
49. Wyld L, et al. The influence of hypoxia and pH on aminolaevulinic acid-induced photodynamic therapy in bladder cancer cells in vitro. *British Journal of Cancer* 1998;vol. 77:1621–1627. [PubMed: 9635837]
50. Georgakoudi I, et al. Hypoxia significantly reduces aminolaevulinic acid-induced protoporphyrin IX synthesis in EMT6 cells. *British Journal of Cancer* 1999;vol. 79:1372–1377. [PubMed: 10188878]
51. Wyld L, et al. Cell cycle phase influences tumour cell sensitivity to aminolaevulinic acid-induced photodynamic therapy in vitro. *British Journal of Cancer* 1998;vol. 78:50–55. [PubMed: 9662250]
52. Ickowicz Schwartz D, et al. Differentiation-dependent photodynamic therapy regulated by porphobilinogen deaminase in B16 melanoma. *British Journal of Cancer* 2004;vol. 90:1833–1841. [PubMed: 15150593]
53. Kremer P, et al. Intraoperative Fluorescence Staining of Malignant Brain Tumors Using 5-Aminofluorescein-Labeled Albumin. *Neurosurgery* 2009 Mar;vol. 64:S53–S61.
54. Iyer AK, et al. Exploiting the enhanced permeability and retention effect for tumor targeting. *Drug Discovery Today* 2006;vol. 11:812–818. [PubMed: 16935749]
55. Murray KJ. A preliminary study. Improved surgical resection of human brain tumors: Part 1. *Surgical Neurology* 1982;vol. 17:316–319. [PubMed: 6283688]
56. Koc K, et al. Fluorescein sodium-guided surgery in glioblastoma multiforme: a prospective evaluation. *Br J Neurosurg* 2008 Feb;vol. 22:99–103. [PubMed: 18224529]
57. Okuda T, et al. Metastatic Brain Tumor Surgery Using Fluorescein Sodium: Technical Note. *Minim Invasive Neurosurg* 2007;vol. 50:382–384. [PubMed: 18210365]
58. Shinoda J, et al. Fluorescence-guided resection of glioblastoma multiforme, by using high-dose fluorescein sodium - Technical note. *Journal of Neurosurgery* 2003 Sep;vol. 99:597–603. [PubMed: 12959452]
59. Uzuka T, et al. Surgical strategy for malignant glioma resection with intraoperative use of fluorescein Na. *Neurological Surgery* 2007 Jun;vol. 35:557–562. [PubMed: 17564048]

60. Kuroiwa T, et al. Development of a Fluorescein Operative Microscope for use During Malignant Glioma Surgery: A Technical Note and Preliminary Report. *Surgical Neurology* 1998;vol. 50:41–49. [PubMed: 9657492]
61. Moore GE, et al. The clinical use of fluorescein in neurosurgery: The localization of brain tumors. *Journal of Neurosurgery* 1948;vol. 5:392–398. [PubMed: 18872412]
62. Hansen DA, et al. Indocyanine Green (Icg) Staining and Demarcation of Tumor Margins in a Rat Glioma Model. *Surgical Neurology* 1993 Dec;vol. 40:451–456. [PubMed: 7694381]
63. Haglund MM, et al. Enhanced Optical Imaging of Rat Gliomas and Tumor Margins. *Neurosurgery* 1994 Nov;vol. 35:930–940. [PubMed: 7838344]
64. Haglund MM, et al. Enhanced optical imaging of human gliomas and tumor margins. *Neurosurgery* 1996 Feb;vol. 38:308–317. [PubMed: 8869058]
65. Britz GW, et al. Intracarotid RMP-7 enhanced indocyanine green staining of tumors in a rat glioma model. *Journal of Neuro-Oncology* 2002 Feb;vol. 56:227–232. [PubMed: 12061728]
66. Chan WCW, et al. Luminescent quantum dots for multiplexed biological detection and imaging. *Current Opinion in Biotechnology* 2002 Feb;vol. 13:40–46. [PubMed: 11849956]
67. Dubertret B, et al. In vivo imaging of quantum dots encapsulated in phospholipid micelles. *Science* 2002 Nov 29;vol. 298:1759–1762. [PubMed: 12459582]
68. Muhammad O, et al. Macrophage-mediated colocalization of quantum dots in experimental glioma. *Methods Mol Biol* 2007;vol. 374:161–171. [PubMed: 17237538]
69. Jackson H, et al. Quantum dots are phagocytized by macrophages and colocalize with experimental gliomas. *Neurosurgery* 2007 Mar;vol. 60:524–529. discussion 529-30. [PubMed: 17327798]
70. Arndt-Jovin DJ, et al. Tumor-Targeted Quantum Dots Can Help Surgeons Find Tumor Boundaries. *IEEE Trans Nanobioscience*. 2009 Mar 16;
71. Wang J, et al. Receptor-targeted quantum dots: fluorescent probes for brain tumor diagnosis. *J Biomed Opt* 2007 Jul–Aug;vol. 12:044021. [PubMed: 17867825]
72. Cai W, et al. Peptide-Labeled Near-Infrared Quantum Dots for Imaging Tumor Vasculature in Living Subjects. *Nano Letters* 2006;vol. 6:669–676. [PubMed: 16608262]
73. Singh S, Nalwa HS. Nanotechnology and health safety - Toxicity and risk assessments of nanostructured materials on human health. *Journal of Nanoscience and Nanotechnology* 2007 Sep;vol. 7:3048–3070. [PubMed: 18019130]
74. Choi HS, et al. Renal clearance of quantum dots. *Nature Biotechnology* 2007 Oct;vol. 25:1165–1170.
75. Sarin H, et al. Effective transvascular delivery of nanoparticles across the blood-brain tumor barrier into malignant glioma cells. *Journal of Translational Medicine* 2008 Dec;vol. 6
76. Orringer DA, et al. In Vitro Characterization of a Targeted, Dye-Loaded Nanodevice for Intraoperative Tumor Delineation. *Neurosurgery* 2009 May;vol. 64:965–971. [PubMed: 19404156]
77. Barry SE. Challenges in the development of magnetic particles for therapeutic applications. *International Journal of Hyperthermia* 2008;vol. 24:451–466. [PubMed: 18608583]
78. Islam T, Josephson L. Current state and future applications of active targeting in malignancies using superparamagnetic iron oxide nanoparticles. *Cancer Biomarkers* 2009;vol. 5:99–107. [PubMed: 19414927]
79. Kircher MF, et al. A Multimodal Nanoparticle for Preoperative Magnetic Resonance Imaging and Intraoperative Optical Brain Tumor Delineation. *Cancer Research* 2003 December 1;vol. 63:8122–8125. 2003. [PubMed: 14678964]
80. Gupta AK, Gupta M. Synthesis and surface engineering of iron oxide nanoparticles for biomedical applications. *Biomaterials* 2005 Jun;vol. 26:3995–4021. [PubMed: 15626447]
81. Trehin R, et al. Fluorescent nanoparticle uptake for brain tumor visualization. *Neoplasia* 2006 Apr;vol. 8:302–311. [PubMed: 16756722]
82. Veisheh O, et al. Inhibition of Tumor-Cell Invasion with Chlorotoxin-Bound Superparamagnetic Nanoparticles. *Small* 2009 Jan;vol. 5:256–264. [PubMed: 19089837]
83. Veisheh O, et al. Optical and MRI multifunctional nanoprobe for targeting gliomas. *Nano Letters* 2005 Jun;vol. 5:1003–1008. [PubMed: 15943433]

84. Sun C, et al. In vivo MRI detection of gliomas by chlorotoxin-conjugated superparamagnetic nanoprobes. *Small* 2008 Mar;vol. 4:372–379. [PubMed: 18232053]
85. Patel MM, et al. Getting into the brain: approaches to enhance brain drug delivery. *CNS Drugs* 2009;vol. 23:35–58. [PubMed: 19062774]
86. Andersson C, et al. Identification of Tissue Sites for Increased Albumin Degradation in Sarcoma-Bearing Mice. *Journal of Surgical Research* 1991 Feb;vol. 50:156–162. [PubMed: 1990221]
87. Stehle G, et al. Plasma protein (albumin) catabolism by the tumor itself - implications for tumor metabolism and the genesis of cachexia. *Critical Reviews in Oncology/Hematology* 1997 Jul;vol. 26:77–100. [PubMed: 9298326]
88. Wunder A, et al. Enhanced albumin uptake by rat tumors. *International Journal of Oncology* 1997 Sep;vol. 11:497–507.
89. Kremer P, et al. Laser-induced fluorescence detection of malignant gliomas using fluorescein-labeled serum albumin: Experimental and preliminary clinical results. *Neurological Research* 2000 Jul;vol. 22:481–489. [PubMed: 10935221]
90. Torp SH, et al. Epidermal Growth-Factor Receptor Expression in Human Gliomas. *Cancer Immunology Immunotherapy* 1991 Mar;vol. 33:61–64.
91. Gibbs-Strauss SL, et al. Diagnostic detection of diffuse glioma tumors in vivo with molecular fluorescent probe-based transmission spectroscopy. *Medical Physics* 2009 Mar;vol. 36:974–983. [PubMed: 19378758]
92. Davis SC, et al. Magnetic resonance-coupled fluorescence tomography scanner for molecular imaging of tissue. *Review of Scientific Instruments* 2008 Jun;vol. 79:064302. [PubMed: 18601421]
93. Weissleder R, et al. In vivo imaging of tumors with protease-activated near-infrared fluorescent probes. *Nature Biotechnology* 1999 Apr;vol. 17:375–378.
94. McCann CM, et al. Combined magnetic resonance and fluorescence imaging of the living mouse brain reveals glioma response to chemotherapy. *Neuroimage* 2009 Apr;vol. 45:360–369. [PubMed: 19154791]
95. Mammen M, et al. Polyvalent interactions in biological systems: Implications for design and use of multivalent ligands and inhibitors. *Angewandte Chemie-International Edition* 1998;vol. 37:2755–2794.
96. Chen X, et al. In vivo Near-Infrared Fluorescence Imaging of Integrin $\alpha_v\beta_3$ in Brain Tumor Xenografts. *Cancer Research* 2004 November 1;vol. 64:8009–8014. 2004. [PubMed: 15520209]
97. Hsu AR, et al. In vivo near-infrared fluorescence imaging of integrin $\alpha_v\beta_3$ in an orthotopic glioblastoma model. *Molecular Imaging & Biology* 2006 Nov–Dec;vol. 8:315–323. [PubMed: 17053862]
98. Kantelhardt SR, et al. Multiphoton excitation fluorescence microscopy of 5-aminolevulinic acid induced fluorescence in experimental gliomas. *Lasers in Surgery & Medicine* 2008 Apr;vol. 40:273–281. [PubMed: 18412229]
99. Hoyt CC, et al. Remote biomedical spectroscopic imaging of human artery wall. *Lasers in Surgery & Medicine* 1988;vol. 8:1–9. [PubMed: 3352449]
100. Tamura Y, et al. Endoscopic identification and biopsy sampling of an intraventricular malignant glioma using a 5-aminolevulinic acid-induced protoporphyrin IX fluorescence imaging system. Technical note. *Journal of Neurosurgery* 2007 Mar;vol. 106:507–510. [PubMed: 17367078]
101. Wagnieres GA, et al. In vivo fluorescence spectroscopy and imaging for oncological applications. *Photochem Photobiol* 1998 Nov;vol. 68:603–632. [PubMed: 9825692]
102. Utzinger U, Richards-Kortum RR. Fiber optic probes for biomedical optical spectroscopy. *Journal of Biomedical Optics* 2003;vol. 8:121–147. [PubMed: 12542388]
103. Pogue BW, et al. Analysis of Sampling Volume and Tissue Heterogeneity upon the In Vivo Detection of Fluorescence. *J. Biomed. Opt* 2005;vol. 10:41206. [PubMed: 16178630]
104. Pogue BW, Burke GC. Fiber optic bundle design for quantitative fluorescence measurement from tissue. *Appl. Opt* 1998;vol. 37:7429–7436. [PubMed: 18301577]

105. Sinaasappel M, Sterenberg HJCM. Quantification of the hematoporphyrin derivative by fluorescence measurement using dual-wavelength excitation and dual-wavelength detection. *Appl. Opt* 1993;vol. 32:541–548.
106. Sterenberg HJ, et al. Evaluation of spectral correction techniques for fluorescence measurements on pigmented lesions in vivo. *Journal of Photochemistry & Photobiology* 1996 Sep;vol. B - Biology. 35:159–165.
107. Ishihara R, et al. Quantitative spectroscopic analysis of 5-aminolevulinic acid-induced protoporphyrin IX fluorescence intensity in diffusely infiltrating astrocytomas. *Neurologia Medico-Chirurgica* 2007 Feb;vol. 47:53–57. discussion 57. [PubMed: 17317941]
108. Utsuki S, et al. Auditory alert system for fluorescence-guided resection of gliomas. *Neurologia Medico-Chirurgica* 2008 Feb;vol. 48:95–97. discussion 97-8. [PubMed: 18296881]
109. Utsuki S, et al. Possibility of using laser spectroscopy for the intraoperative detection of nonfluorescing brain tumors and the boundaries of brain tumor infiltrates. Technical note. *J Neurosurg* 2006 Apr;vol. 104:618–620. [PubMed: 16619668]
110. Yang VXD, et al. A multispectral fluorescence imaging system: design and initial clinical tests in intra-operative Photofrin-photodynamic therapy of brain tumors. *Lasers in Surgery & Medicine* 2003;vol. 32:224–232. [PubMed: 12605430]
111. Kuroiwa T, et al. Comparison between operative findings on malignant glioma by a fluorescein surgical microscopy and histological findings. *Neurological Research* 1999 Jan;vol. 21:130–134. [PubMed: 10048072]
112. Stummer W, et al. Technical principles for protoporphyrin-IX-fluorescence guided microsurgical resection of malignant glioma tissue. *Acta Neurochirurgica* 1998;vol. 140:995–1000. [PubMed: 9856241]
113. Gebhart SC, et al. Liquid-crystal tunable filter spectral imaging for brain tumor demarcation. *Applied Optics* 2007 Apr 1;vol. 46:1896–1910. [PubMed: 17356636]
114. Yang VX, et al. A multispectral fluorescence imaging system: design and initial clinical tests in intra-operative Photofrin-photodynamic therapy of brain tumors. *Lasers Surg Med* 2003;vol. 32:224–232. [PubMed: 12605430]
115. Davis SC, et al. Magnetic resonance-coupled fluorescence tomography scanner for molecular imaging of small animals and human breasts. *Rev. Sci. Instr.* 2008 (submitted).
116. DeAngelis LM. Brain tumors. *N Engl J Med* 2001 Jan 11;vol. 344:114–123. [PubMed: 11150363]
117. Wen PY, Kesari S. Malignant gliomas in adults. *N Engl J Med* 2008 Jul 31;vol. 359:492–507. [PubMed: 18669428]
118. Michotte A, et al. Neuropathological and molecular aspects of low-grade and high-grade gliomas. *Acta Neurol Belg* 2004 Dec;vol. 104:148–153. [PubMed: 15742604]
119. Bondy ML, et al. Brain tumor epidemiology: consensus from the Brain Tumor Epidemiology Consortium. *Cancer* 2008 Oct 1;vol. 113:1953–1968. [PubMed: 18798534]
120. Albert FK, et al. Early postoperative magnetic resonance imaging after resection of malignant glioma: objective evaluation of residual tumor and its influence on regrowth and prognosis. *Neurosurgery* 1994 Jan;vol. 34:45–60. discussion 60-1. [PubMed: 8121569]
121. Barker FG 2nd, et al. Radiation response and survival time in patients with glioblastoma multiforme. *J Neurosurg* 1996 Mar;vol. 84:442–448. [PubMed: 8609556]
122. Lacroix M, et al. A multivariate analysis of 416 patients with glioblastoma multiforme: prognosis, extent of resection, and survival. *J Neurosurg* 2001 Aug;vol. 95:190–198. [PubMed: 11780887]
123. Pichlmeier U, et al. Resection and survival in glioblastoma multiforme: an RTOG recursive partitioning analysis of ALA study patients. *Neuro Oncol* 2008 Dec;vol. 10:1025–1034. [PubMed: 18667747]
124. Stummer W, et al. Extent of resection and survival in glioblastoma multiforme: identification of and adjustment for bias. *Neurosurgery* 2008 Mar;vol. 62:564–576. discussion 564-76. [PubMed: 18425006]
125. Vecht CJ, et al. The influence of the extent of surgery on the neurological function and survival in malignant glioma. A retrospective analysis in 243 patients. *J Neurol Neurosurg Psychiatry* 1990 Jun;vol. 53:466–471. [PubMed: 2166137]

126. Utsuki S, et al. Fluorescence-guided resection of metastatic brain tumors using a 5-aminolevulinic acid-induced protoporphyrin IX: pathological study. *Brain Tumor Pathol* 2007;vol. 24:53–55. [PubMed: 18095131]
127. Utsuki S, et al. Histological examination of false positive tissue resection using 5-aminolevulinic acid-induced fluorescence guidance. *Neurologia Medico-Chirurgica* 2007 May;vol. 47:210–213. discussion 213-4. [PubMed: 17527047]
128. Toda M. Intraoperative navigation and fluorescence imagings in malignant glioma surgery. *Keio Journal of Medicine* 2008 Sep;vol. 57:155–161. [PubMed: 18854668]
129. Morofuji Y, et al. Usefulness of intraoperative photodynamic diagnosis using 5-aminolevulinic acid for meningiomas with cranial invasion: technical case report. *Neurosurgery* 2008 Mar;vol. 62:102–103. discussion 103-4. [PubMed: 18424972]
130. Miyatake S, et al. Fluorescence of non-neoplastic, magnetic resonance imaging-enhancing tissue by 5-aminolevulinic acid: case report. *Neurosurgery* 2007 Nov;vol. 61:E1101–E1103. discussion E1103-4. [PubMed: 18091261]
131. Kajimoto Y, et al. Use of 5-aminolevulinic acid in fluorescence-guided resection of meningioma with high risk of recurrence. Case report. *J Neurosurg* 2007 Jun;vol. 106:1070–1074. [PubMed: 17564181]
132. Hefti M, et al. 5-aminolevulinic acid induced protoporphyrin IX fluorescence in high-grade glioma surgery: a one-year experience at a single institution. *Swiss Med Wkly* 2008 Mar 22;vol. 138:180–185. [PubMed: 18363116]
133. Valdes P, et al. Brain tumor resection guided by fluorescence imaging and MRI image guidance. *Medical Imaging 2009: Visualization, Image-Guided Procedures, and Modeling, Proceedings of SPIE Vol. 7261 2009:726103*. in " in.
134. Leblond F, et al. Brain tumor resection guided by fluorescence imaging. *Proceedings of the SPIE - The International Society for Optical Engineering 2009*;vol. 7164:8.
135. Miyatake, S-i, et al. Fluorescence of non-neoplastic, magnetic resonance imaging-enhancing tissue by 5-aminolevulinic acid: case report. *Neurosurgery* 2007 Nov;vol. 61:E1101–E1103. discussion E1103-4. [PubMed: 18091261]
136. Stummer W, et al. Fluorescence-guided resections of malignant gliomas--an overview. *Acta Neurochirurgica - Supplement* 2003;vol. 88:9–12. [PubMed: 14531555]
137. Eljamel MS, et al. ALA and Photofrin fluorescence-guided resection and repetitive PDT in glioblastoma multiforme: a single centre Phase III randomised controlled trial. *Lasers Med Sci* 2008 Oct;vol. 23:361–367. [PubMed: 17926079]

Biographies



Brian W. Pogue, Ph.D. received his B.Sc. Honors degree and M.Sc. degrees from York University, Canada in 1989 and 1991 respectively. He completed his Ph.D. in Physics from McMaster University in 1995 and a postdoctoral research at the Wellman Center for Photomedicine at the Massachusetts General Hospital from 1995–96. He joined the Thayer School of engineering in 1996 and is currently Professor of Engineering Sciences, with adjunct appointments in Surgery and Physics and Astronomy at Dartmouth. He is currently Dean of Graduate Studies at Dartmouth and directs research in the areas of optical spectroscopy of cancer, imaging research, and imaging cancer pathobiology. He is Deputy

editor of *Optics Letters* and Associate Editor for *Medical Physics*, the *Journal of Biomedical Optics* and the *Journal of Photochemistry and Photobiology B*.



Summer L. Gibbs-Strauss completed her B.S. in biochemistry at Whitworth College in 2003, and then completed her Ph.D. at the Thayer School of Engineering at Dartmouth College in 2008. Her thesis work was on the methodology assessment of fluorescence imaging of glioma tumors with endogenous and exogenous contrast agents, specifically examining the accuracy for detection and therapy monitoring of micro-invasive xenograft models as compared to bulk tumors. She is currently a Research Fellow at the Beth Israel Deaconess Medical Center in the Harvard Medical School working on the development of near-infrared fluorescent contrast agents and near-infrared fluorescence image-guided surgery.



Pablo A. Valdes completed his B.S. in chemistry at the Florida International University in 2005, and is currently enrolled in the M.D./Ph.D. Program at Dartmouth College. He has completed 2 years of his M.D. training, and is currently in his 2nd year of the Ph.D. program at the Thayer School of Engineering at Dartmouth. His work focuses on fluorescence guided brain tumor resection and analysis of protoporphyrin IX production mechanisms in vivo. His advisors are Keith D. Paulsen and David W. Roberts.



Kimberley S. Samkoe completed her B.Sc. Honors at the University of Regina, Canada in 2001, and Ph.D. in Biophysical Chemistry and the University of Calgary in 2007. Her thesis work was in the field of photodynamic therapy using two photon excitation, and

examination of biological damage in vasculature examined in ovo. She is currently a post-doctoral research associate at the Thayer School of Engineering at Dartmouth College in the field of photodynamic therapy and fluorescence optical tomography for cancer imaging, and carries out research analyzing treatment efficacy with Magnetic Resonance Imaging and optical tomography.



David W. Roberts received his M.D. degree from Dartmouth Medical School in 1975 and completed an internship in General Surgery at the University of Utah School of Medicine in 1975–76, followed by a residency in Neurosurgery at Dartmouth-Hitchcock Medical Center, 1978–1982. He is the section chief of Neurosurgery and complete research in stereotactic neurosurgery, epileptic disorders, movement disorders and brain tumors. He is a member of the Norris Cotton Cancer Center Neuro-Oncology Program as well as the Cell Imaging and Radiobiology Research Program. He directs an NIH funded research project into fluorescence guided neurosurgery for glioma tumors.



Keith D. Paulsen received the B.S. degree in biomedical engineering from Duke University, Durham, NC, in 1981, and the M.S. and Ph.D. degrees from Dartmouth College, Hanover, in 1984 and 1986, respectively. He is the Robert A. Pritzker Chair in Biomedical Engineering at the Thayer School of Engineering, Dartmouth College, Hanover, NH. He is also a Professor of radiology at Dartmouth Medical School, Dartmouth Hitchcock Medical Center, Lebanon, NH, where he is also the Director of the Advanced Imaging Center. He is also the Co-Director of the Cancer Imaging and Radiobiology Research Program at Norris Cotton Cancer Center, Lebanon. His current research interests include in cancer imaging techniques in the breast and brain. He has authored or coauthored over 200 articles published in peer-reviewed scientific and medical literature. Prof. Paulsen has received

numerous awards for funding his research from the National Institutes of Health. He is an Associate Editor of IEEE Transactions on Medical Imaging.

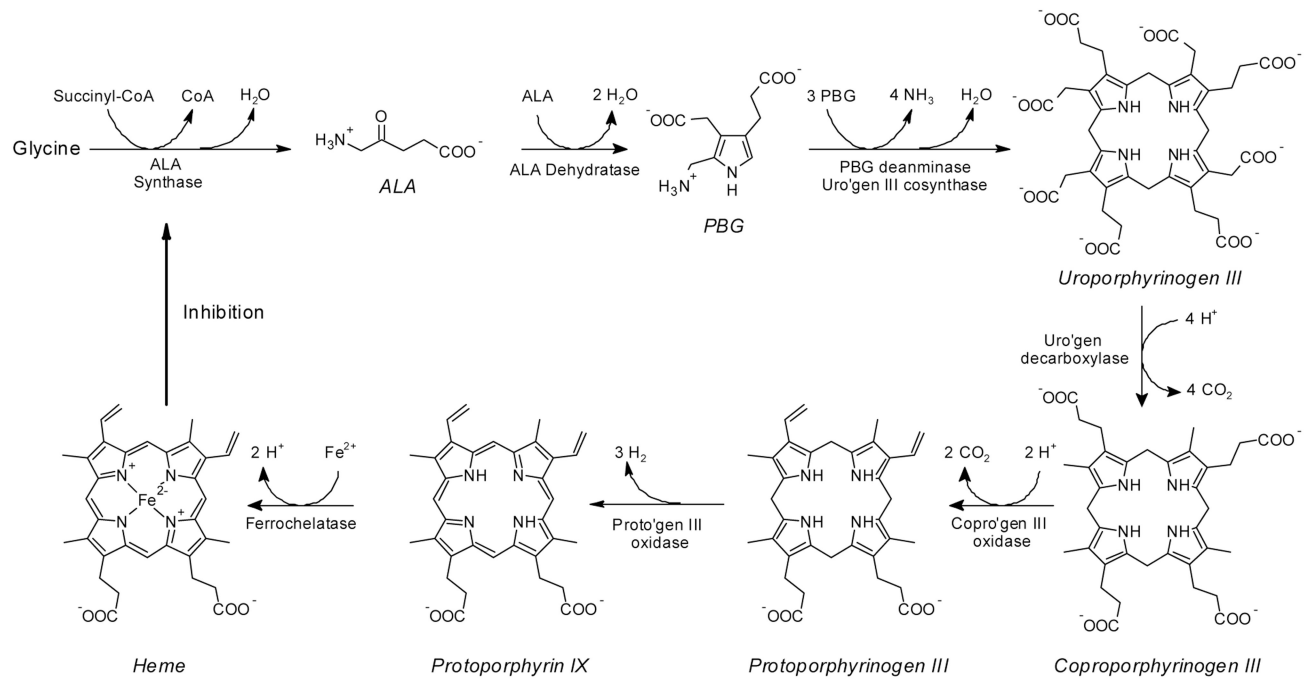


Fig. 1. The biochemical steps in the heme synthesis pathway, which occurs in and around the mitochondria of all mammalian cells at varying levels of production [10].

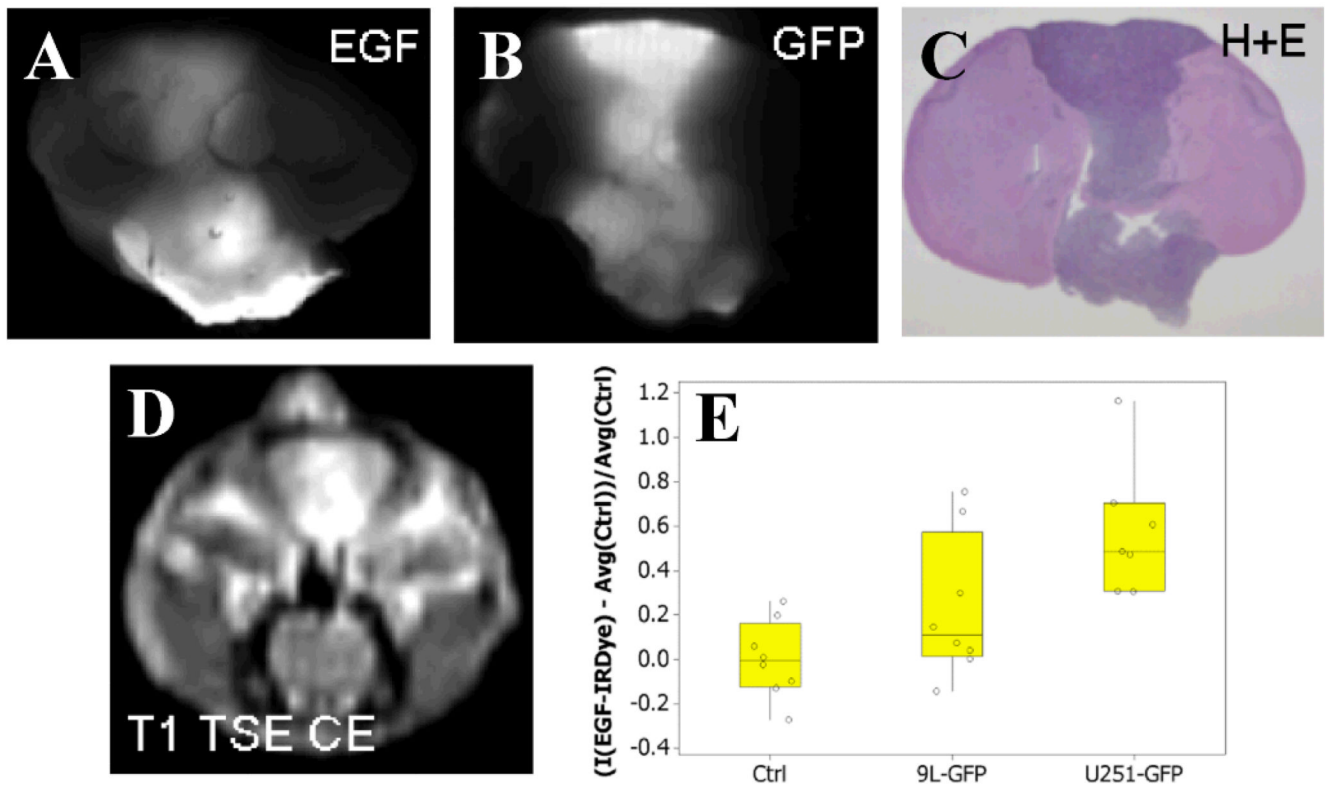


Fig. 2. Administration of the exogenous EGF conjugated IRDye 800CW in mice bearing orthotopic gliomas allows tumor boundary demarcation ex vivo and diagnosis in vivo. This example demonstrates that in a 9L-GFP mouse model the fluorescence from the EGF-IRDye 800CW conjugate (A) corresponds well with the GFP fluorescence from 9L transfected cells (B), H&E histological staining (C), and standard T1-weighted TSE contrast enhanced MRI (D). Additionally, using in vivo fluorescence transmission imaging it was found that mice bearing tumors could be detected with success over mice without tumors.

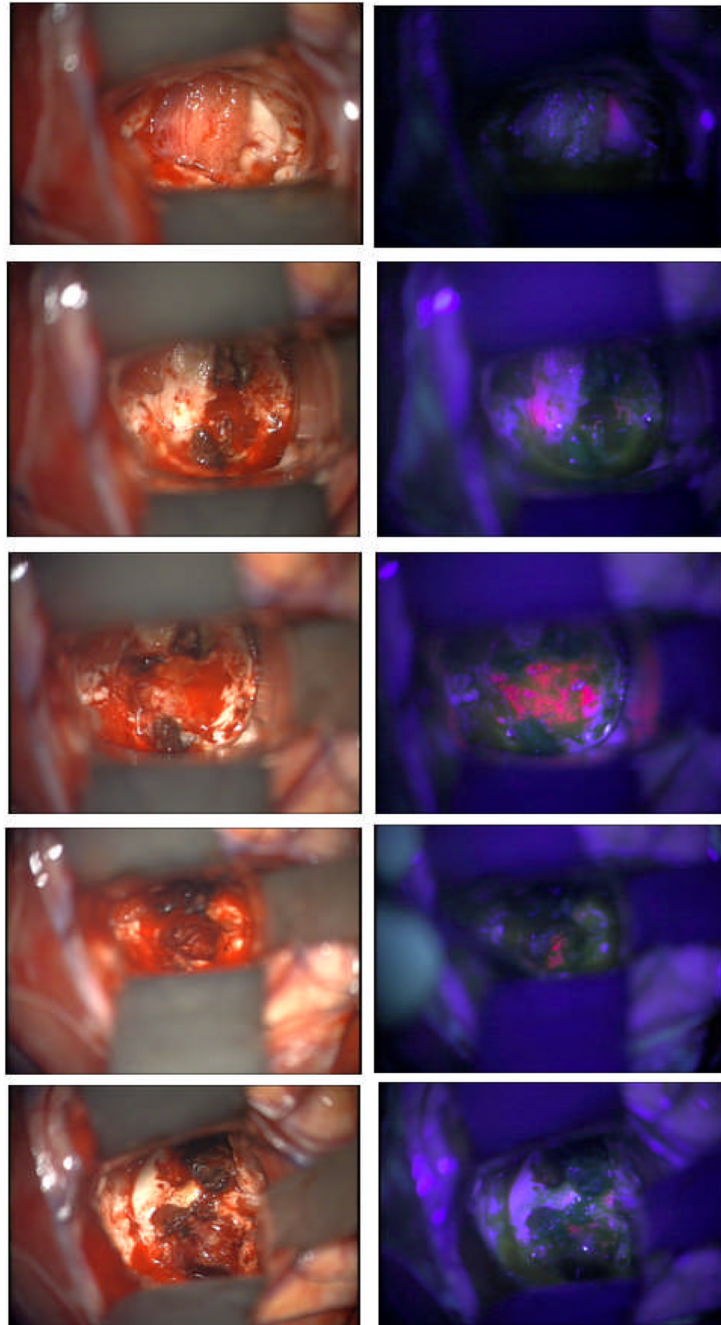


Fig. 3. Resection imaging of a glioma tumor during surgery, with white light (left column) and ALA-PpIX fluorescence (right column). The PpIX appears as the pink fluorescence, and is visualized by blue excitation light, with appropriate filtering.

TABLE I

Environmental Factors affecting PpIX Production from ALA

Influencing Factor	Effect on PpIX Production	Reference(s)
Low Glucose	↑	[48]
High Glucose	↓	[48]
Hypoxia	↓	[49–50]
Normal Oxygen Levels	↑	[49–50]
Low Incubation Temperature	↓	[12]
High Incubation Temperature	↑	[12]
Acidic pH	↓	[32,49]
Neutral pH	↑	[32,49]
Basic pH	↓	[32,49]
Plateau Growth Phase	↑	[38]
Exponential Growth Phase	↓	[38]
High Plating Density	↑	[40,50]
Low Plating Density	↓	[40,50]
G ₂ + M Cell Cycle Phase	↑	[40,51]
G ₁ Cell Cycle Phase	↓	[40]
Differentiation Therapy	↑	[45,52]